

Functional Orderly Topography of Brain Networks Associated with Gene Expression Heterogeneity

Wei Liu

College of Intelligence Science and Technology, National University of Defense Technology

Lingli Zeng

College of Intelligence Science and Technology, National University of Defense Technology

Hui Shen

National University of Defense Technology

Zongtan Zhou

College of Intelligence Science and Technology, National University of Defense Technology

dewen hu (✉ dwhu@nudt.edu.cn)

College of Intelligence Science and Technology, National University of Defense Technology

Article

Keywords: cerebral cortex, brain networks, neocortex, nuclei, cognitive functions

Posted Date: October 11th, 2021

DOI: <https://doi.org/10.21203/rs.3.rs-944509/v1>

License: © ⓘ This work is licensed under a Creative Commons Attribution 4.0 International License. [Read Full License](#)

Version of Record: A version of this preprint was published at Communications Biology on October 11th, 2022. See the published version at <https://doi.org/10.1038/s42003-022-04039-8>.

Abstract

The human cerebral cortex expanded much more relative to non-human primates and rodent in evolution, leading to a functional orderly topography of the brain networks. Here, we show that functional topography may be associated with gene expression heterogeneity in various brain structures. The neocortex exhibits greater gene expression heterogeneity, with lower housekeeping gene proportion, a longer mean path length, less clusters, and a lower degree of ordering of networks, compared to archicortical and subcortical area in human, rhesus macaque, and mouse brains consistently. In particular, the cerebellar cortex displays greater gene expression heterogeneity than cerebellar deep nuclei in the human brain, but not in the mouse brain, corresponding to the emergence of novel functions in the human cerebellar cortex. Moreover, the cortical areas with greater gene expression heterogeneity, primarily located in multimodal association cortex, tend to express genes with higher evolutionary rates and exhibit higher functional connectivity degree measured by resting-state fMRI, implying that such spatial pattern of cortical gene expression may be shaped by evolution and favorable for the specialization of higher cognitive functions. Together, the cross-species imaging genetic findings may provide convergent evidence to support the association between the orderly topography of brain function networks and gene expression.

Introduction

The human brain has been developed a hierarchical organization infrastructure that remains among mammals in topographically some extents of similar, including the neocortex, archicortex, and subcortical areas, according to the origin age of the evolutionary history^{1,2}. On this basis, almost mammalian brains demonstrate orderly topography in the functional networks, in which higher cognitive functions are primarily fulfilled by the neocortex, rather than the archicortical and subcortical areas^{3,4}. The spatial and topological layout of functional brain networks are highly heritable, likely due to genome blueprint⁵⁻⁷. However, the underlying molecular architecture to support such functional topography of brain structures is little understood.

While retaining the basic layout of cortical areas that can be traced back to the homologous regions of the rodent and non-human primate brain, the human brain has undergone remarkable changes in the process of evolution, with the human cerebral cortex is vastly expanded relative to non-human primates and rodent, and disproportionately occupied by multimodal association areas^{8,9}. The multimodal association areas and their structural and functional connections in the human brain, primarily constituting the cognitive functional networks, such as the frontoparietal network, salience network, and default-mode network, play an essential role in higher-order brain functions^{10,11}. Most previous studies suggest that the development of higher-order cognitive networks in recent human brain evolution are associated with specific gene expression profiles^{12,13}. However, the pattern of gene expression in the human brain to support the emergence of its unique functions remains unresolved.

The availability of genome-wide spatially mapped gene expression data provides a great opportunity to understand the relationship between gene expression and the anatomical and functional organization of the mammalian brain¹⁴⁻¹⁷. Over the past decade, a number of transcriptome studies focusing on region-related changes in human brain gene expression profiles were published. Recent studies performing resting-state functional magnetic resonance imaging (fMRI) have revealed that functional connectivity networks can be

recapitulated using correlated gene expression in a post-mortem brain sample¹⁸. Further studies reported that some genes could influence connectivity strength between network hubs of the human connectome¹⁹ and some genes could play a role in the expansion of higher-order cognitive networks⁷ using comparative transcriptomics analysis. These findings imply that the emergence of orderly functional networks in the human brain may be the result of changes at the genetic level.

We hypothesized that there might be gene expression heterogeneity in various brain structures associated with the functional orderly topography of brain networks. Here, we speculated the heterogeneity of gene expression in brain structures, including the proportion of housekeeping genes occupying all expressed genes and topology indexes of gene expression networks. Housekeeping genes (HKGs) are usually expressed at relative constant rates for the basic molecular and cellular function of neurons²⁰, thus the lower proportion of HKGs expressed in brain structures may suggest its higher functional diversity. Topology indexes of gene expression networks in brain structures, including mean path length, clustering coefficient and eigen entropy, offer possibilities to understand how genes work together to perform diverse functions²¹. Especially, we compared the heterogeneity of gene expression in multimodal association areas with that of unimodal primary cortex in the human brain to investigate the role of gene expression in the functional specialization of human evolution. Then, we studied the association of the heterogeneity of brain structures and the hierarchical architecture of functional connectivity networks, to reveal the basic principle by which the brain is organized throughout the evolution history at least across the rodent, rhesus macaque, and human.

Results

HKG expression proportion is lower in the neocortex than that in the archicortex and subcortex. We constructed gene expression networks for all brain samples by combining human gene expression from the Allen Institute for Brain Science (<http://human.brain-map.org/>) and large-scale protein interaction data (see the Methods section). The gene expression data were obtained from six adult brains (two contributed both hemispheres, and four contributed one hemisphere), for a total of 3,702 brain samples²². Considering the diversity among the different subjects, we analyzed and compared the gene expression networks between samples within a given human brain. Based on the gene expression networks, we extracted the percentages of HKGs and specific genes, which were expressed in almost all samples²³ and expressed in only one or two samples, respectively²⁴.

The percentages of HKGs are mapped to the samples of Brain #1 (Fig. 1a). The samples with relatively low percentages of HKGs were primarily located in the neocortex of the human brain. Compared to the archicortex and subcortex, the neocortex in the human brain performs diverse and complex functions, and thus likely requires more expressed genes in addition to HKGs. Similar results were obtained in the other five human brains (Supplementary Fig. 1 and Supplementary Table 1). As shown in Fig. 1b, the HKG percentages in the neocortex in Brain #1 were significantly lower than those in the archicortex and subcortex (Both P -values < 0.001 in two sample t -test). Not surprisingly, the genes expressed in the neocortex tend to have lower gene expression levels and higher expression specificity than those in the archicortex and subcortex (Supplementary Table 1).

The HKG percentages were mapped to the main structures in Brain #1 (Fig. 1c). Interestingly, the cerebellum exhibited a relatively lower mean HKG percentage than the cerebral nuclei, interbrain, and brainstem. However, after dividing the cerebellum into interior structures, significant differences were observed in the HKG

percentages between the cerebellar cortex and cerebellar deep nuclei. The cerebellar cortex, including the lateral hemisphere ($33.60 \pm 1.58\%$) and paravermis ($33.61 \pm 1.76\%$), exhibited a lower HKG percentage than the cerebellar deep nuclei ($39.70 \pm 4.74\%$). Thus, significant expression difference may exist between the different structures of the cerebellum, coinciding with their functions. According to previous studies, the cerebellum in humans not only plays an important role in motor control, which is mainly executed by the cerebellar deep nuclei, but also is involved in certain higher-order cognitive functions, such as attention and language, which are executed by the cerebellar cortex^{25, 26}.

To investigate the relationship of the HKG percentage and evolution, we analyzed the evolutionary rate of expressed genes (see the Methods section) to measure the selective constraints to which the brain regions were subjected. As shown in Fig. 1d, the HKG percentages in the samples of Brain #1 were found to decrease as the average evolutionary rates of the expression genes increase. Similar results can be observed in the other five brains. These results imply that the brain regions with lower HKG percentages show higher average evolutionary rate under less evolutionary pressure, compared the other regions.

Newly developed brain regions exhibit increased heterogeneity in their internal expression networks. To analyze the gene expression heterogeneity from a network perspective, we computed three typical topological indexes of gene expression networks, including the mean path length, clustering coefficient and eigen entropy, to measure the overall navigability, modularity, and orderness of the networks (see the Methods section and Supplementary Table 2). In general, a longer mean path length, smaller clustering coefficient and larger eigen entropy of a network may suggest that it is sparser, containing less clusters and more disorderly, and thus shows greater heterogeneity of gene expression.

The gene expression networks in the neocortex exhibited greater heterogeneity, with longer mean path lengths, smaller clustering coefficients and larger eigen entropies, than those in the archicortex and subcortex (Fig. 2ab). Meanwhile, significant correlations were observed among the three topological indexes and average evolutionary rate of genes. We found that the mean path lengths in the brain samples increase as the average evolutionary rates of genes increase, as shown in Fig. 2c. Our results revealed that the orderness of the gene expression networks in the brain regions presented a downward trend according to the evolution order of the brain regions, consistent with the evolution theory of life systems that the development of organisms and a highly complex brain is a process of diminishing entropy^{27, 28}. The results obtained from the six brains were consistent.

Brain regions with greater expression heterogeneity were primarily located in multimodal association cortex of the human brain. To investigating the heterogeneity of internal structures in the neocortex, we integrated the gene expression data of brain samples from six adult individuals through the standard process described in previous studies²⁹ (see Supplementary Methods for details) and mapped them to seven networks of cerebral cortex³⁰. According to the gene expression heterogeneity, seven brain networks showed orderly topography from multimodal association cortex to unimodal primary cortex. The multimodal association cortex including frontoparietal control, attention, and default networks showed lower gene expression similarity within networks than the visual, motor, and limbic networks (Fig. 3a, see the Methods section), while the higher-order cognitive functional networks consistently exhibited more differences in gene expression compared with the visual and motor networks (Fig. 3b). Meanwhile, the gene expression similarity within networks was found positively

correlated with the corresponding standard error of gene expression levels ($R=0.87$, $P=0.01$). The multimodal association cortex possessed lower standard error of gene expression levels compared with the unimodal primary cortex, implying its gene expression is more unbalanced, as shown in Fig. 3c. These results indicated that the multimodal association cortex exhibited greater expression heterogeneity, not only in the lower expression similarity within networks, but also the greater dispersion degree of gene expression levels.

Brain regions with greater expression heterogeneity tend to be connected to more regions in the functional connectivity networks. To explore whether genes with highly consistent cortical patterns across individuals drive this functional organization, we compared the gene expression with resting-state functional connectivity MRI data from the Human Connectome Project^{31,32}. We generated a region-level functional connectivity matrix C averaged across 50 subjects using linear correlations of 116 regions from the automated anatomical labeling (AAL) atlas³³ (see the Methods section). Then, we computed the topological properties of the functional connectivity networks in the human brain, including the degree and betweenness coefficient of each brain region.

We compared the properties of the gene expression networks with those of the functional connectivity networks in the human brain. The degree of brain regions in the functional connectivity networks was negatively correlated with the HKG percentage ($R=-0.39$, -0.25 , -0.31 , -0.20 , -0.20 , and -0.33 for Brains #1-6, respectively, all with $P<0.01$) and positively correlated with the mean path length of gene expression network ($R=0.35$, 0.31 , 0.37 , 0.16 , 0.25 , and 0.32 for Brains #1-6, respectively, $P<0.01$). Thus, brain regions connected to more regions in the functional connectivity networks are primarily located in the neocortex of the human brain and tend to exhibit greater expression heterogeneity, with lower proportions of HKGs and longer mean path lengths in their expression networks (Fig. 4 and Supplementary Fig. 2). These results suggested that the brain regions with greater expression heterogeneity tend to be closely related to each other, in order to perform more interdependent functions.

The gene expression patterns in the mouse and rhesus macaque brain are similar to that in the human brain. Subsequently, based on the expression data from Allen Institute mouse brain atlas from a 56-day-old male C57BL/6J mouse brain³⁴ and protein interactions in the mouse brain, we established gene expression networks in 73 structures of the adult mouse brain (see the Method, Supplementary Table 3). Mouse brain regions with lower HKG proportions tended to be newly developed, as shown in Fig. 5a. Focused on the isocortex of the mouse brain, the 'Perirhinal area' exhibited the lowest percentage of HKGs, followed by the 'Prelimbic area', with values of 29.17% and 30.76% (Supplementary Fig. 3), consistent with those of previous evolutionary analyses across species³⁵. Especially, mouse cerebellum owns the highest HKG proportion (44.90%), suggesting that there may be significant evolutionary differences in the cerebellum between humans and mice³⁶. We found the mean path length and eigen entropy of the gene expression networks in the isocortex (4.09 ± 0.09 and 5.13 ± 0.10 , respectively) were significantly higher than those in the cerebral nuclei (3.83 ± 0.10 and 4.96 ± 0.05 , respectively), indicating the brain structures that evolved later exhibit greater heterogeneity than those that evolved earlier. Based on resting-state functional MRI data of forty-eight male C57BL/6J mice^{37,38}, we established the functional connectivity networks of the mouse brains (see the Methods section) and found the negative correlation between the HKG percentage in gene expression and region degree in functional connectivity networks ($R=-0.53$, $P=0.01$, Fig. 5b), confirmed the results obtained from the human brains.

Furthermore, we generated the expression networks by integrating the gene expression data of the adult rhesus macaque specimen from the NIH Blueprint Non-Human Primate Atlas⁴⁰ with interaction data from STRING database, and the functional connectivity networks based on monkey functional MRI data (see Method and Supplementary Table 4). We found the gene expression networks in neocortex tend to own greater heterogeneity, with lower HKG percentage, longer mean path length and higher functional degree, than those in archicortex and subcortex (Fig. 5cd), in line with the results obtained from human brain.

Discussion

Our combined comparative neuroimaging and genetic findings suggest that heterogeneity changes in the gene expression may play an important role in the formation of the functional topography in the human brain. Based on the multi-resolution gene expression networks in human brains at the sample, structure and region levels, and those in rhesus macaque and mouse brains, the heterogeneity of gene expression in the neocortex was found to be significantly greater than those in the archicortex and subcortex, associated with the functional orderly topography of brain networks. The results obtained from the different resolution networks and different individuals are consistent, indicating that such gene expression pattern in brains is robust and inherent. Especially, the increased heterogeneity of gene expression in multimodal association areas potentially serves the specialization of higher-order cognitive functions in the human brain evolution, compatible with prior observations of high expression of evolution-related genes in these brain areas⁷.

The increased heterogeneity of gene expression networks from the archicortex and subcortex to neocortex was found closely correlated with the average evolutionary rate of expressed genes, indicating that the spatial architecture of gene expression is very likely the product of natural selection. Similarly, its associated functional orderly topography of the brain is commonly believed to be shaped under the pressure of evolution^{11,41}. The structures in the neocortex expressed more non-HKGs to perform their complex functions under the short-term evolutionary pressure, while the structures in the archicortex and subcortex reduced their proportion of specific expressed genes to maintain the stability of their functions under the long-term evolutionary pressure. Such an organization mode of brain networks can ensure that the functions of neocortical areas are implemented effectively and flexibly, while the critical functions of archicortical and subcortical areas are performed steadily and systematically.

Our analyses further showed that more expression of non-HKGs in the neocortex were associated with the change of topological properties of the gene expression networks. Characterization of the human brain from a network perspective has become a powerful tool for inspecting the structural and functional architectures of the brain^{41,42}. The regions in the neocortex exhibited significantly different topological properties both in gene expression networks and functional connectivity networks compared with those in the archicortex and subcortex, indicating that greater expression heterogeneity may support their stronger functional diversity. Meanwhile, our comparative analyses showed that the cognitive functional networks exhibited higher similarity in gene expression among them, but differences compared with the sensorimotor networks, supporting the notion about the large cortical expansion of associative prefrontal, temporal, and parietal areas in the human brain relative to other mammals^{43,44}.

In this study, we observed the similar orderly topology of gene expression heterogeneity in the human, rhesus macaque, and mouse brains. However, the distributions of gene expression heterogeneity in brain structures of rhesus macaques and mice are not completely consistent with that of humans. For example, human cerebellar cortex displayed greater gene expression heterogeneity than cerebellar deep nuclei, which has not been observed in the mouse brain. Such human-distinct patterns in spatial gene expression may imply emerging cognitive functions in the human cerebellar cortex^{25,26}, underlying the differences in cognitive abilities between human and other mammals.

Due to the limitation of brain sampling resolution in different species, this study mainly focused on the global intraspecies differences of gene expression heterogeneity in brain structures, while interspecies regional-matched differences need to be analyzed when more datasets are available. At the same time, individual differences were observed in the gene expression characteristics and topological properties between the structure of different individuals within the species. Therefore, differences among brains must be further investigated when the gene expression data of more individuals become available.

Methods

Constructing gene expression networks in samples of human brains. If two genes were expressed in a given brain sample and available in the integrated human protein interaction network, then both genes were included in the gene expression network of the sample. The integrated protein interaction dataset was established by merging the previous material⁴⁵ with the iRefIndex database⁴⁶ (Supplementary Table 5). By integrating the expression data and large-scale protein interaction data, we established gene expression networks for samples from six human brains.

Computation of the evolutionary rate. The evolutionary rate is a measurement used to quantify the speed of evolutionary change. We calculated the dN/dS values for all genes expressed in the human brains to characterize their evolutionary rates. The synonymous and non-synonymous substitution rates between human and mouse were obtained from Ensembl (<http://www.ensembl.org/biomart/martview/>).

Topological properties of networks. The mean path length represents the average of the shortest paths between all pairs of nodes and offers a measure of a network's overall navigability⁴⁷. In addition, the average clustering coefficient characterizes the overall tendency of the nodes to form clusters or groups⁴⁸. The eigen entropy of networks was defined as the entropy of the normalized largest eigen vector of an adjacency matrix²⁸ (see Supplementary Methods for details).

Gene expression similarity within and between networks. The similarity of gene expression within a network is defined as the mean value of the correlation coefficient of gene expression between any two samples from this network. The similarity of gene expression between networks is defined as the mean value of the correlation coefficient of gene expression between a pair of samples from two different networks.

Functional connectivity of human brains. Functional connectivity was analyzed using resting-state functional MRI data from 50 randomly selected subjects from the Human Connectome Project (HCP, <http://www.humanconnectome.org/documentation/S500/>). The HCP minimal preprocessing pipeline was used for the resting-state fMRI data⁴⁹, which includes artifact removal, motion correction⁵⁰, and registration to a

standard space (see Supplementary Methods for details). The AAL atlas, which divided the whole brain into 116 regions, was used for the region-to-region functional connectivity measures in the current study³³. We evaluated the functional connectivity between each pair of regional averaged time courses using Pearson's correlation coefficient. Significant functional correlations were selected using one-sample *t*-tests ($P < 0.05$, Bonferroni correction), resulting in the binary 116×116 symmetric connectivity matrix *C* of the functional connectivity network in human brains (Supplementary Table 6).

Functional connectivity of mouse brains. Resting-state fMRI data of anesthetized mice were collected from fifty male C57BL/6J mice (Janvier, Le Genest-St Isle, France) between 10 and 13 weeks old weighing 30.6 ± 1.9 g (mean + SD), which are publicly available on the central.xnat.org repository in Analyze 7.5 format (Project ID: fMRI_ane_mouse). Then, the following steps were performed: 1) slice timing correction; 2) motion correction; 3) normalization with an in-house EPI template; 4) spatial smoothing using a 0.4-mm full width half-maximum Gaussian kernel; 5) linear detrending and band-pass temporal filtering (0.01–0.3 Hz); 6) regression of nuisance variables, including the six parameters obtained by rigid body head motion correction, global signals, and their first temporal derivatives. The functional connectivity between each pair of regional averaged time courses was evaluated using Pearson's correlation coefficient. Significant functional correlations were selected to obtain the binary 22×22 symmetric connectivity matrix of the functional connectivity network in mouse brains (Supplementary Table 7).

Functional connectivity of adult rhesus macaque brains. The monkey fMRI data were from PRIME-DE, an open resource for non-human primate imaging (http://fcon_1000.projects.nitrc.org/indi/indiPRIME.html)⁵¹. The image data were collected from a group of 12 male anesthetized rhesus macaque monkeys in University of Western Ontario^{52,53}. The resting-state experiments were conducted on a 7T MRI scanner equipped with a 40-cm gradient coil set of 80 mT/m strength, and a custom-made 24-channel phased array receive coil with an 8-channel transmit coil was used. Resting-state images were acquired using a 2-dimensional multi-band and EPI sequence. The preprocessing steps were performed using SPM8 For each monkey. The first 10 time points were dismissed to account for magnetic saturation. Then, the following steps were then performed: 1) slice timing correction; 2) motion correction; 3) normalization with the INIA19 template (1.0-mm isotropic voxels)⁵⁴; 4) spatial smoothing using a 2-mm full width half-maximum Gaussian kernel; 5) linear detrend and band-pass temporal filtering (0.01–0.3 Hz); 6) regression of nuisance variables, including the six parameters obtained by rigid body head motion correction, global signal, and their first temporal derivatives. Based on D99 template of macaque brain³⁴, we selected significant functional correlations to obtain the binary 304×304 symmetric connectivity matrix of the functional connectivity network in macaque brains (Supplementary Table 8).

Declarations

Code availability

Any custom code or software used to analyze the gene expression characteristics and the topological properties of networks detailed in this study will be made available upon request.

Data availability

The expression data used in this study are available via the Allen Institute for Brain Atlas (see <http://brain-map.org/>). The interactions in human, rhesus macaque and mouse are available in Supplementary Table 7, STRING and BIOGRID database. Resting-state fMRI data of human, rhesus macaque, and mouse can be found in <http://www.humanconnectome.org/documentation/S500/>, http://fcon_1000.projects.nitrc.org/indi/indiPRIME.html, and central.xnat.org, respectively. The authors declare that the data supporting the findings of this study are available within the article, its supplementary information, and upon request.

Competing interests

The authors have no competing interests to declare.

References

1. Kaas, J. H. The evolution of brains from early mammals to humans. *Wiley Interdiscip Rev. Cogn. Sci.* **4(1)**, 33-45 (2013).
2. Molnár, Z. et al. Evolution and development of the mammalian cerebral cortex. *Brain Behav. Evol.* **83(2)**, 126-139 (2014).
3. Betzel, R. F. & Bassett, D. S. Multi-scale brain networks. *Neuroimage* **160**, 73-83 (2017).
4. Sjöstedt, E. et al. An atlas of the protein-coding genes in the human, pig, and mouse brain. *Science* **367(6482)**, eaay5947 (2020).
5. Bae, B., Jayaraman, D. & Walsh, C. A. Genetic changes shaping the human brain. *Dev. Cell* **32(4)**, 423-434 (2015).
6. Vallender, E. J. Genetics of human brain evolution. *Progress in Brain Research* **250**, 3-39 (2019).
7. Wei, Y. et al. Genetic mapping and evolutionary analysis of human-expanded cognitive networks. *Nat. Commun.* **10(1)**, 4839 (2019).
8. Hofman, M. A. Evolution of the human brain: when bigger is better. *Front. Neuroanat.* **8**, 15 (2014).
9. Xu, T. et al. Cross-species functional alignment reveals evolutionary hierarchy within the connectome. *Neuroimage* **223**, 117346 (2020).
10. Park, H. J. & Friston, K. Structural and functional brain networks: from connections to cognition. *Science* **342(6158)**, 1238411 (2013).
11. Buckner, R. L. & Krienen, F. M. The evolution of distributed association networks in the human brain. *Trends Cogn. Sci.* **17(12)**, 648-665 (2013).
12. Hawrylycz, M. et al. Canonical genetic signatures of the adult human brain. *Nat. Neurosci.* **18(12)**, 1832-1846 (2015).
13. Wang, W. & Wang, G. Z. Understanding molecular mechanisms of the brain through transcriptomics. *Front. Physiol.* **10**, 214 (2019).
14. Kang, H. J. et al. Spatio-temporal transcriptome of the human brain. *Nature* **478(7370)**, 483-489 (2011).
15. Lein, E. S. et al. Genome-wide atlas of gene expression in the adult mouse brain. *Nature* **445(7124)**, 168-177 (2007).

16. Wang, D. et al. Comprehensive functional genomic resource and integrative model for the human brain. *Science* **362(6420)**, eaat8464 (2018).
17. Mahfouz A. et al. Brain transcriptome atlases: a computational perspective. *Brain Struct Funct.* **222(4)**, 1557–1580 (2017).
18. Richiardi, J. et al. Correlated gene expression supports synchronous activity in brain networks. *Science* **348(6240)**, 1241-1244 (2015).
19. Arnatkeviciute A. et al. Genetic influences on hub connectivity of the human connectome. *Nat. Commun.* **12(1)**, 4237 (2021).
20. Butte, A. J., Dzau, V. J. & Glueck, S. B. Further defining housekeeping, or "maintenance," genes Focus on "A compendium of gene expression in normal human tissues". *Physiological genomics* **7(2)**, 95-96 (2001).
21. Krienen, F. M., Yeo, B.T.T., Ge, T., Buckner, R. L. & Sherwood, C. C. Transcriptional profiles of supragranular-enriched genes associate with corticocortical network architecture in the human brain. *Proc Natl Acad Sci U S A* **113(4)**, E469-78 (2016).
22. Hawrylycz, M. J. et al. An anatomically comprehensive atlas of the adult human brain transcriptome. *Nature* **489(7416)**, 391-399 (2012).
23. Emig, D. & Albrecht, M. Tissue-specific proteins and functional implications. *J. Proteome Res.* **10(4)**, 1893-1903 (2011).
24. Dezso, Z. et al. A comprehensive functional analysis of tissue specificity of human gene expression. *BMC Biology* **6**, 49 (2008).
25. Hu, D., Shen, H. & Zhou, Z. Functional asymmetry in the cerebellum: a brief review. *Cerebellum* **7(3)**, 4-13 (2008).
26. Schmahmann J. D. The cerebellum and cognition. *Neurosci Lett.* **688**, 62-75 (2019).
27. Yao, Y. et al. The increase of the functional entropy of the human brain with age. *Sci. Rep.* **3**, 2853 (2013).
28. Fan, Y., Zeng, L. L., Shen, H., Qin, J., Li, F. Q. & Hu, D. W. Lifespan development of the human brain revealed by large-scale network eigen-entropy. *Entropy* **19(9)**, 471 (2017).
29. Arnatkevic, I. A., Fulcher, B. D. & Fornito, A. A practical guide to linking brain-wide gene expression and neuroimaging data. *Neuroimage* **189**, 353-367 (2019).
30. Yeo, B.T., et al. The organization of the human cerebral cortex estimated by intrinsic functional connectivity. *Journal of Neurophysiology* **106**, 1125-1165 (2011).
31. Van Essen, D. C. et al. The WU-Minn Human Connectome Project: an overview. *Neuroimage* **80**, 62-79 (2013).
32. Smith, S. M. et al. Resting-state fMRI in the Human Connectome Project. *Neuroimage* **80**, 144-168 (2013).
33. Tzourio-Mazoyer, N. et al. Automated anatomical labeling of activations in SPM using a macroscopic anatomical parcellation of the MNI MRI single-subject brain. *Neuroimage* **15(1)**, 273-289 (2002).
34. Ng, L. et al. An anatomic gene expression atlas of the adult mouse brain. *Nat. Neurosci.* **12(3)**, 356-362 (2009).
35. Bradbury, J. Molecular insights into human brain evolution. *PLoS Biol.* **3(3)**, e50 (2005).
36. Haldipur, P. et al. Spatiotemporal expansion of primary progenitor zones in the developing human cerebellum. *Science* **366(6464)**, 454-460 (2019).

37. Zerbi, V., Grandjean, J., Rudin, M. & Wenderoth, N. Mapping the mouse brain with rs-fMRI: An optimized pipeline for functional network identification. *NeuroImage* **123**, 11-21 (2015).
38. Schroeter, A., Schlegel, F., Seuwen, A., Grandjean, J. & Rudin, M. Specificity of stimulus-evoked fMRI responses in the mouse: the influence of systemic physiological changes associated with innocuous stimulation under four different anesthetics. *NeuroImage* **94**, 372-384 (2014).
39. Reveley, C. et al. Three-dimensional digital template atlas of the macaque brain. *Cereb. Cortex* **27(9)**, 4463-4477 (2017).
40. Bakken, T. E. et al. A comprehensive transcriptional map of primate brain development. *Nature* **535(7612)**, 367-375 (2016).
41. Liao, X., Vasilakos, A. V. & Yong, H. Small-world human brain networks: Perspectives and challenges. *Neurosci. Biobehav. Rev.* **77**, 286-300 (2017).
42. Seguin, C., van den Heuvel, M. P. & Zalesky, A. Navigation of brain networks. *Proc. Natl Acad. Sci. USA* **115(24)**, 6297-6302 (2018).
43. Hill, J. et al. Similar patterns of cortical expansion during human development and evolution. *Proc. Natl Acad. Sci. USA* **107**, 13135–13140 (2010).
44. Donahue, C. J., Glasser, M. F., Preuss, T. M., Rilling, J. K. & Van Essen, D. C. Quantitative assessment of prefrontal cortex in humans relative to nonhuman primates. *Proc. Natl Acad. Sci. USA* **115**, E5183–E5192 (2018).
45. Bossi A, Lehner B. Region specificity and the human protein interaction network. *Molecular Systems Biology* **5**, 260 (2009).
46. Razick S, Magklaras G, Donaldson IM. iRefIndex: a consolidated protein interaction database with provenance. *BMC Bioinformatics* **9**, 405 (2008).
47. Barabasi, A. L. & Oltvai Z. N. Network biology: understanding the cell's functional organization. *Nat. Rev. Genet.* **5(2)**, 101-113 (2004).
48. Milo, R., Shen-Orr, S., Itzkovitz, S., Kashtan, N., Chklovskii, D. & Alon, U. Network motifs: simple building blocks of complex networks. *Science* **298(5594)**, 824-827 (2002).
49. Craddock, R. C., James, G. A., Holtzheimer, P. E., Hu, X. P. & Mayberg, H. S. A whole brain fMRI atlas generated via spatially constrained spectral clustering. *Hum. Brain Mapp.* **33(8)**, 1914-1928 (2012).
50. Zeng, L. L. et al. Neurobiological basis of head motion in brain imaging. *Proc. Natl Acad. Sci. USA* **111(16)**, 6058-6062 (2014).
51. Milham, M. P. et al. An open resource for non-human primate imaging. *Neuron* **100(1)**, 61-74 (2018).
52. Gilbert, K. M., Gati, J. S., Barker, K., Everling, S. & Menon, R. S. Optimized parallel transmit and receive radiofrequency coil for ultrahigh-field MRI of monkeys. *Neuroimage* **125**, 153-161 (2016).
53. Ghahremani, M., Hutchison, R. M., Menon, R. S. & Everling, S. Frontoparietal functional connectivity in the common marmoset. *Cereb. Cortex* **27(8)**, 3890-3905 (2017).
54. Rohlfing, T. et al. The INIA19 template and NeuroMaps atlas for primate brain image parcellation and spatial normalization. *Front Neuroinform.* **6**, 27 (2012).

Figures

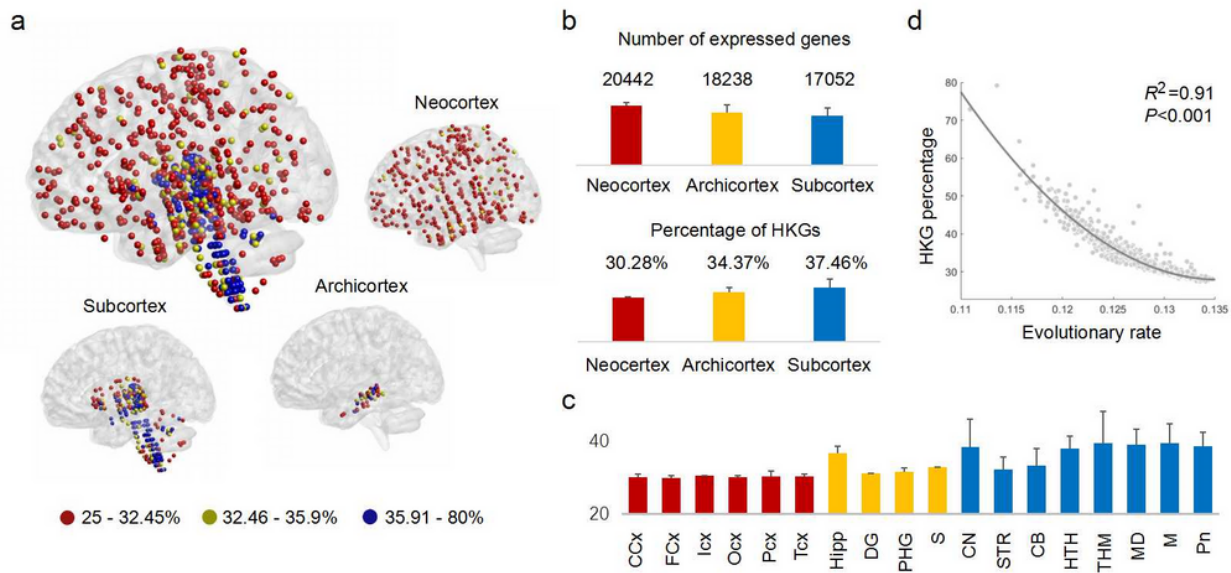


Figure 1

Gene expression characteristics in the human brain samples. a, The percentage of HKGs mapped to the brain samples of Brain #1. The proportion of HKG expression to that of other specific genes was considerably higher in the archicortex and subcortex than that in the neocortical areas. b, The mean value and standard deviation of the expressed gene number and HKG percentage in the neocortex, archicortex and subcortex of Brain #1. c, The percentage of HKGs mapped to the main structures of Brain #1. The structures in the neocortex, archicortex and subcortex are marked in red, yellow and blue, respectively. CCx: Cingulate neocortex; FCx: Frontal neocortex; lcx: Insular neocortex; Ocx: Occipital neocortex; PCx: Parietal neocortex; TCx: Temporal neocortex; Hipp: Hippocampal proper; DG: Dentate area; PHG: Parahippocampal gyrus; S: Subiculum; CN: Cerebral nuclei; STR: Striatum; CB: Cerebellum; HTH: Hypothalamus; THM: Thalamus; MD: Medulla; M: Midbrain; Pn: Pons. d, The average evolutionary rate of expressed genes was negatively correlated with the HKG percentage in the samples of Brain #1.

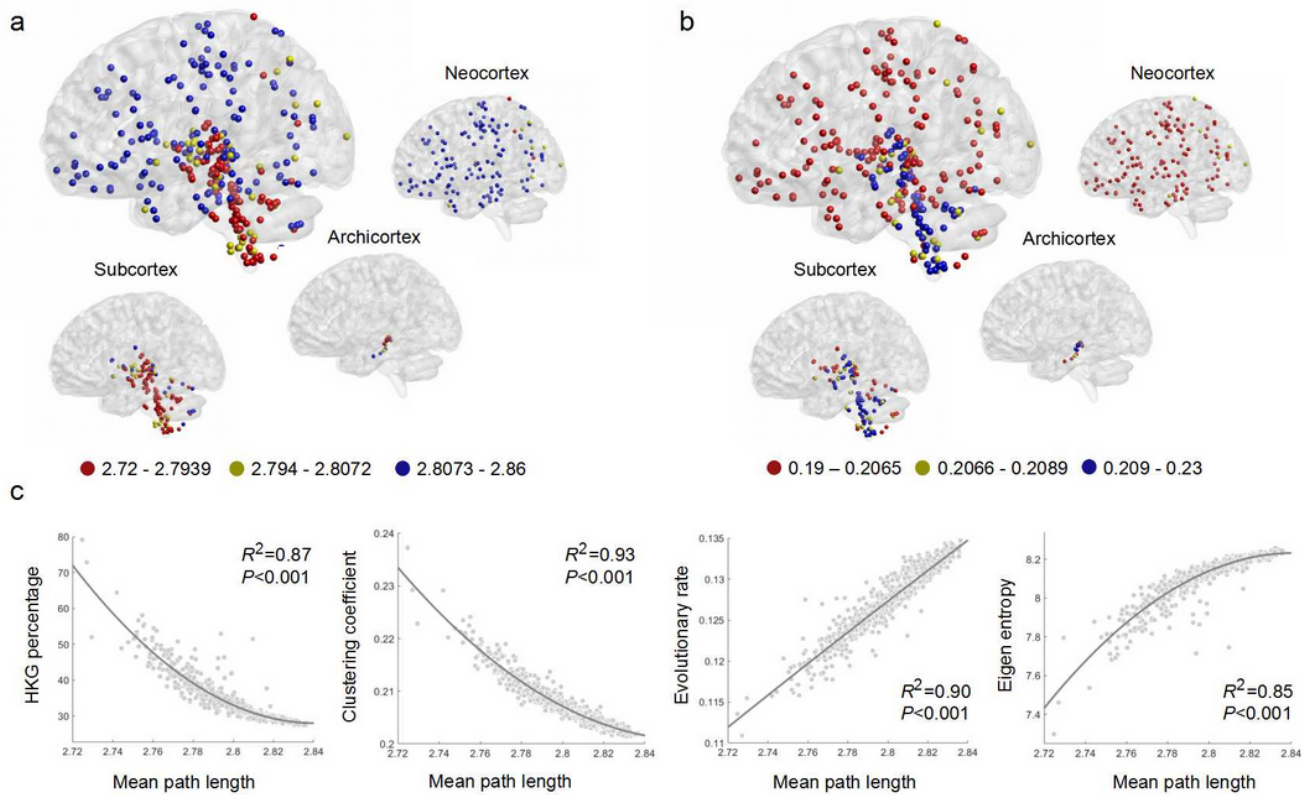


Figure 2

The topological properties of gene expression networks and their relationships. a, The mean path length and b, clustering coefficient mapped to all brain structures in Brain #1. The gene expression networks in the neocortex have longer mean path lengths and smaller clustering coefficients than those in the archicortex and subcortex. c, The mean path length was negatively correlated with the HKG percentage and clustering coefficient and positively correlated with the evolutionary rate of expressed genes and eigen entropy of gene expression networks in the samples of Brain #1.

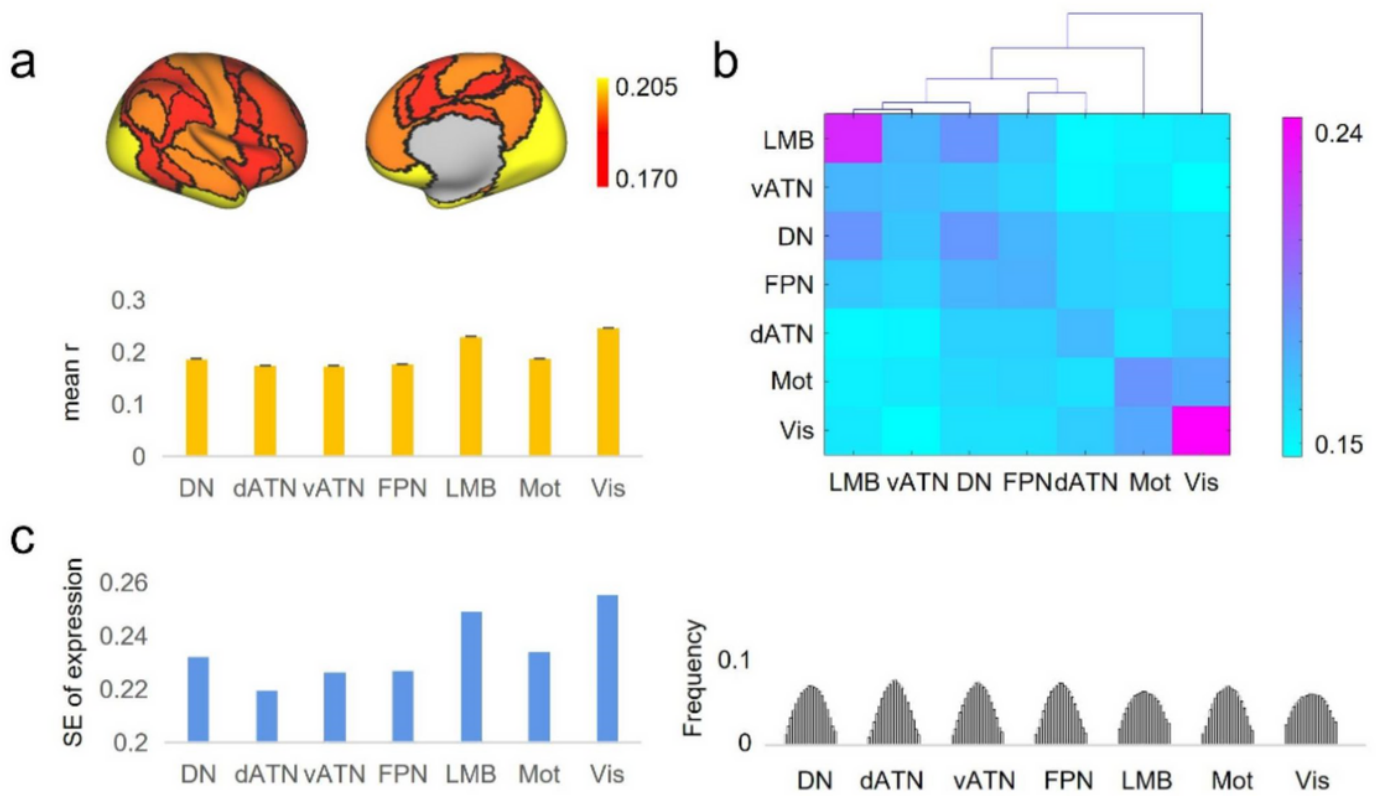


Figure 3

The expression heterogeneity of seven networks in human cerebral cortex. a, Mean correlation coefficient of gene expression of samples within each network. b, The hierarchical clustering of gene expression between networks. c, The standard error of gene expression levels in samples of each network and their corresponding distribution. DN: default mode network; dATN: dorsal attention network; vATN: ventral attention network; FPN: frontal parietal network; LMB: limbic network; Mot: motion network; Vis: visual network.

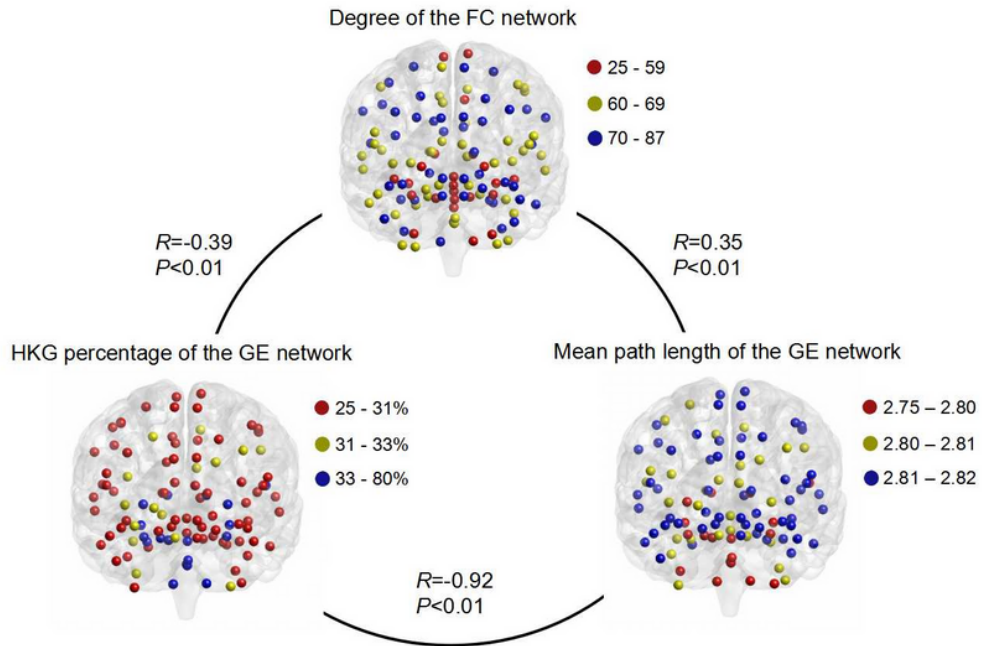


Figure 4

Comparison of gene expression networks and the functional connectivity network in human brains. The degree of the functional connectivity network was significantly negatively correlated with the HKG percentage and positively correlated with the mean path length of the gene expression network in Brain #1. FC, functional connectivity; GE, gene expression.

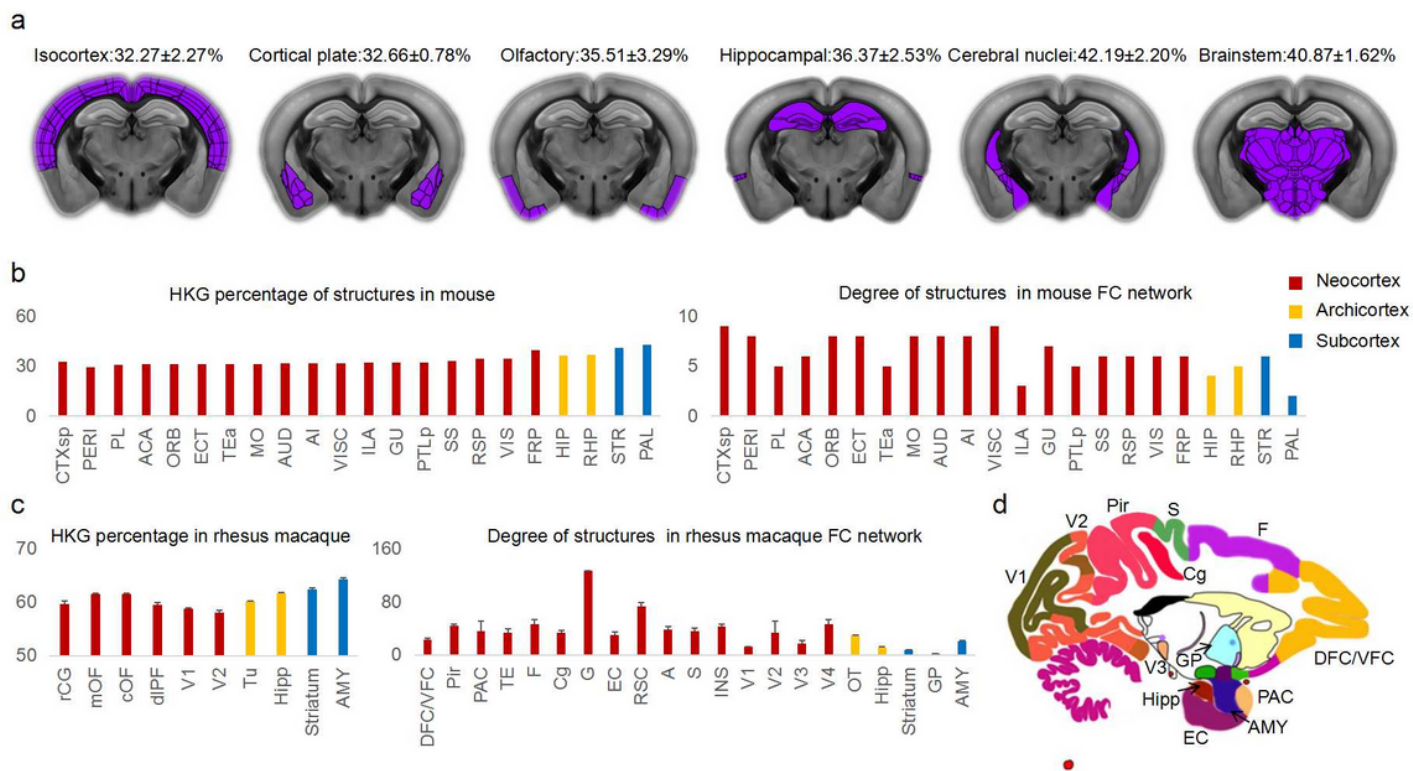


Figure 5

Comparison of the gene expression network and the functional connectivity network in the mouse and rhesus macaque brain. a, The HKG percentages mapped to mouse brain regions. The HKG percentage in the neocortex is lower than those in the archicortex (including the olfactory area and hippocampal formation) and subcortex (cerebral nuclei and brainstem). The regions of interest are marked in purple. All hybridization images were obtained from the Allen Mouse Brain Atlas. b, The HKG percentage of gene expression and the degree of functional connectivity in mouse brain structures. c, The HKG percentage of gene expression and the degree of functional connectivity in rhesus macaque brain structures. d, The diagram of main structures in rhesus macaque brain. This picture is generated based on the D99 brain template³⁹. The description of brain structures can be found in Supplementary Methods.

Supplementary Files

This is a list of supplementary files associated with this preprint. Click to download.

- [SupplementaryDataandmethods.docx](#)
- [Supplementaryfigure1TheHKGpercentagesinhumanbrains.jpg](#)
- [Supplementaryfigure2Correlationofnetworkpropertiesandfunctionalconnectivity.jpg](#)
- [Supplementaryfigure3HKGpercentagemappedtoisocortexofmousebrain.jpg](#)
- [SupplementaryTable1ThegeneexpressionHKGandspecificgenepercentageofsamplesinsixhumanbrains.xlsx](#)
- [SupplementaryTable2Thenetworkpropertiesofsamplesinsixhumanbrains.xlsx](#)

- [SupplementaryTable3Thehumanproteininteractiondataset.xlsx](#)
- [SupplementaryTable4Thepropertiesofstructuresinthemousebrain.xlsx](#)
- [SupplementaryTable5Thepropertiesofstructuresintherhesusmacaquebrain.xlsx](#)
- [SupplementaryTable6TheZscoresandPvaluesofthefunctionalconnectivitynetworkinhumanbrains.xls](#)
- [SupplementaryTable7TheZscoresandPvaluesofthefunctionalconnectivitynetworkinthemousebrain.xls](#)
- [SupplementaryTable8TheZscoresofthefunctionalconnectivitynetworkintherhesusmacaquebrain.xlsx](#)